Bioorganic & Medicinal Chemistry 20 (2012) 866–876

Contents lists available at SciVerse ScienceDirect

Bioorganic & Medicinal Chemistry

journal homepage: www.elsevier.com/locate/bmc

Pyridobenzothiazole derivatives as new chemotype targeting the HCV NS5B polymerase

Giuseppe Manfroni [a,*], Francesco Meschini [a], Maria Letizia Barreca [a,*], Pieter Leyssen [b], Alberta Samuele [c], Nunzio Iraci [a], Stefano Sabatini [a], Serena Massari [a], Giovanni Maga [c], Johan Neyts [b], Violetta Cecchetti [a]

[a] Dipartimento di Chimica e Tecnologia del Farmaco, University of Perugia, 06123 Perugia, Italy
[b] Rega Institute for Medical Research, Katholieke Universiteit Leuven, B-3000 Leuven, Belgium
[c] Istituto di Genetica Molecolare, IGM-CNR, 27100 Pavia, Italy

ARTICLE INFO

Article history:
Received 9 June 2011
Revised 25 November 2011
Accepted 26 November 2011
Available online 3 December 2011

Keywords:
Hepatitis C
NS5B inhibitors
HCV inhibitors
Pyridobenzothiazole derivatives
Thumb site I
Thumb site II
Molecular docking

ABSTRACT

Hepatitis C virus (HCV) infection has been recognized as the major cause of liver failure that can lead to hepatocellular carcinoma. Among all the HCV proteins, NS5B polymerase represents a leading target for drug discovery strategies. Herein, we describe our initial research efforts towards the identification of new chemotypes as allosteric NS5B inhibitors. In particular, the design, synthesis, in vitro anti-NS5B and in cellulo anti-HCV evaluation of a series of 1-oxo-1*H*-pyrido[2,1-*b*][1,3]benzothiazole-4-carboxylate derivatives are reported. Some of the newly synthesized compounds showed an IC_{50} ranging from 11 to 23 μM, and molecular modeling and biochemical studies suggested that the thumb domain could be the target site for this new class of NS5B inhibitors.

1. Introduction

Chronic hepatitis C virus (HCV) infection is emerging as a major health burden with an estimated 180 million chronically infected individuals worldwide and 3–4 million new cases of infection each year.[1,2] HCV has been found to be a major cause of cirrhosis, hepatocellular carcinoma, as well as liver failure, and is the most common cause of the need for liver transplantation.[3] To date, there is no vaccine available against HCV. The standard treatment is a combination of pegylated interferon-α and ribavirin, a broad spectrum anti-viral agent;[4] this therapy is however aspecific, expensive, poorly tolerated and of limited efficacy in genotype 1 infected patients, who comprise the majority of individuals that are chronically infected in Europe and North America. The development of new, virus-specific, more efficacious, and better tolerated anti-viral agents is therefore of primary importance.[5]

In the last decade, the acquired knowledge of the HCV life cycle and of structural features of the HCV proteins have revealed several targets for the development of potential novel therapeutics and promising direct-acting anti-virals (DAAs)—also named 'specifically targeted anti-viral therapy for hepatitis C' (STAT-C) compounds—have been progressed in phase I to II clinical trials,[6–8] with the NS3/4A protease inhibitors boceprevir (Victrelis™ from Merck)[9] and telaprevir (Incivek™ from Vertex Pharmaceutical),[10] that very recently have reached the market. However, the use of these protease inhibitors still requires the combination with the aspecific pegylated interferon-α and ribavirin drugs. Beside NS3/4A, one of the most interesting targets for the development of DAAs is the viral protein NS5B, a key enzyme in the virus replication cycle having RNA-dependent RNA polymerase activity, a functionality which is not present in human cells thus making the target attractive. The discovery of a drug that targets NS5B polymerase still remains an exciting challenge that would help in the development of an interferon/ribavirin-free HCV therapy, plausibly based on a combination of DAAs acting on different targets to hamper rapid emergence of resistance. The NS5B polymerase offers a wide range of possibilities for the discovery of new molecular entities, since it contains one active site and at least five allosteric drugable sites.[11]

Two main types of NS5B inhibitors have been developed to date:[12–14] nucleoside or nucleotide inhibitors (NIs) which bind the active site of the enzyme, and non-nucleoside inhibitors (NNIs) which target one of the allosteric sites of the enzyme preventing a conformational transition needed for initiation of RNA synthesis.

* Corresponding authors. Tel.: +39 075 585 5126; fax: +39 075 585 5115 (G.M); tel.: +39 075 585 5157; fax: +39 075 585 5115 (M.L.B.).
E-mail addresses: giuseppe.manfroni@unipg.it (G. Manfroni), lbarreca@unipg.it (M.L. Barreca).

0968-0896/$ - see front matter © 2011 Elsevier Ltd. All rights reserved.
doi:10.1016/j.bmc.2011.11.061

As a part of our effort to identify new anti-HCV chemotypes, we have herein focused our attention on the inhibitors binding to the allosteric site referred to as thumb site I (TSI), which is located at the upper section of the thumb domain, approximately 30 Å from the active site. Benzimidazole and indole derivatives represent promising TSI non-nucleoside inhibitors (TSI-NNIs), and they have been the focus of intense lead optimization research at several pharmaceutical companies.[12] As an example, exhaustive structural modifications around the benzimidazole scaffold, performed by Japan Tobacco, led to the identification of candidate JTK-109 (**1**)[15](Fig. 1), a potent and selective inhibitor which was advanced into phase II clinical trials and later terminated for undisclosed reasons.

Herein, a series of pyridobenzothiazole derivatives were designed and synthesized following a scaffold hopping strategy. In vitro anti-NS5B and in cellulo anti-HCV evaluation of the newly synthesized compounds indicate that this chemical class might serve as a good starting point for further lead optimization strategies.

2. Results and discussion

2.1. Rational design

The aim of our work was the identification of new chemotypes as potential TSI-NNIs through the application of a traditional scaffold hopping strategy. Scaffold hopping is a powerful tool to discover structurally novel compounds by modifying the central core structure of known active compounds.[16] Structural and structure–activity relationship (SAR) studies of known TSI-NNIs illustrated in the literature[15,17,18] have pointed out the presence of three key chemical features correlated with the NS5B inhibition

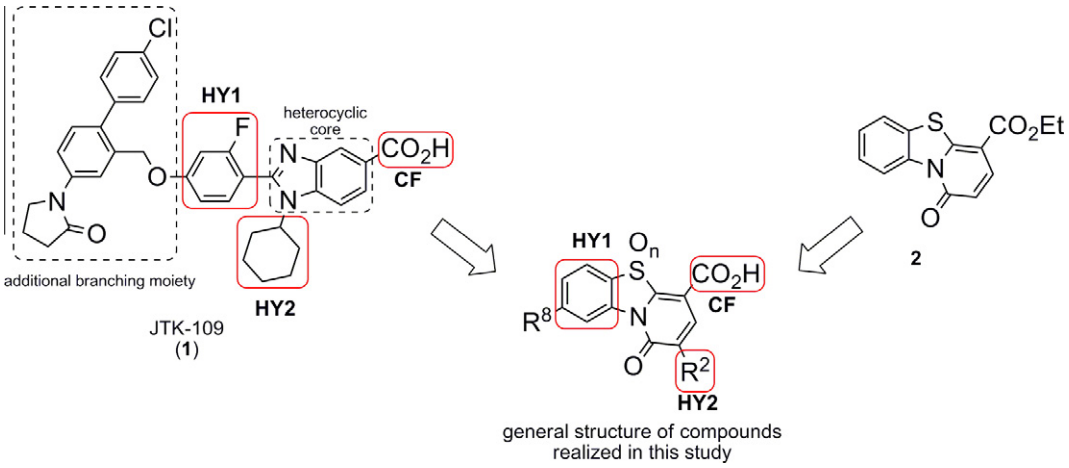

Figure 1. Chemical structure of JTK-109 (**1**) and design concept. The key chemical features are highlighted in red.

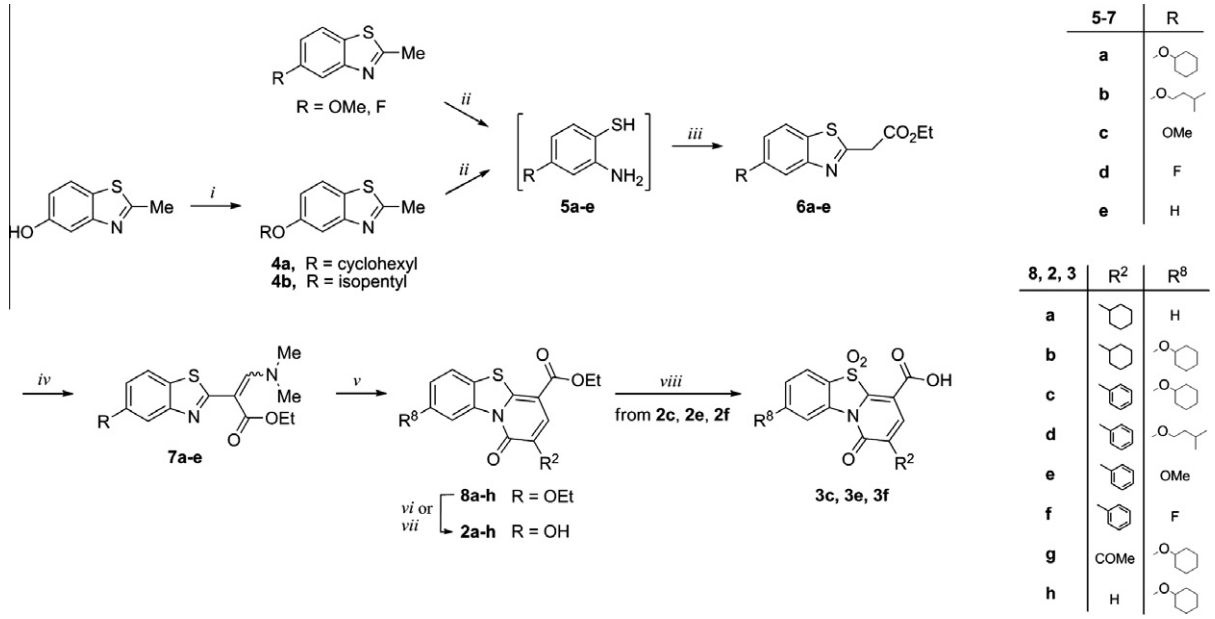

Scheme 1. Reagents and conditions: (i) cyclohexanol or isopentanol, PPh_3, DEAD, TEA, THF, ultrasounds, rt; (ii) 50% NaOH, ethylene glycol, reflux; (iii) ethyl cyanoacetate, 120 °C; (iv) Vilsmeier reagent 90 °C; (v) appropriate anhydrides or diketene 100–110 °C; (vi) 4% NaOH, MeOH, 75 °C; (vii) aqueous 1 N LiOH, MeOH, 40 °C; (viii) *m*-CPBA, CH_2Cl_2, rt.

ability, i.e., two lipophilic portions (HY1 and HY2) and one carboxylic/carbonyl function (CF) able to establish salt bridge/hydrogen bond interaction. These functionalities are maintained in a spatial arrangement suitable for the interaction within the NS5B TSI by a heterocyclic central core, typically an indole or a benzimidazole ring. Additional branching moieties can be present to further optimize potency and/or physiochemical properties. All these chemical regions are illustrated in Figure 1, taking as example the benzimidazole derivative **1**.

Our scaffold hopping drug design of new TSI-NNI chemotypes was primarily focused on the identification of a heterocycle core framework able to replace the central chemical template of bioactive compounds such as **1**, while keeping the above mentioned key interaction features in a spatial orientation appropriate to fit into TSI.

To achieve this goal, a variety of scaffolds was scrutinized by a thorough bibliographic research, looking for a heterocyclic system never employed in the development of anti-HCV compounds, easy to synthesize and suitable for appropriate chemical functionalization. The ethyl 1-oxo-1*H*-pyrido[2,1-*b*][1,3]benzothiazole-4-carboxylate (**2**), reported by Kato et al.[19] seemed to match all the above mentioned requirements (Fig. 1). Indeed, the compound presented an ester group easily hydrolyzable to the necessary CF, and an HY1 portion embedded in the tricyclic system. Moreover, the second required lipophilic area (HY2) could have been easily inserted at the C-2 position adapting the procedure reported by Kato (Fig. 1).

Thus, the pyridobenzothiazole derivatives **2a**–**h**, characterized by a different substitution pattern at C-2 and C-8 positions (Scheme 1 and Table 1), were synthesized. Cyclohexyl (**2a**, **2b**) or phenyl groups (**2c**–**f**) were considered as lipophilic substituents at the C-2 position; C-2 acetyl (**2g**) and C-2 unsubstituted (**2h**) derivatives were also synthesized to further explore the importance of the lipophilic area HY2.

Likewise **1** and its analogues, most of the synthesized pyridobenzothiazoles have an additional aliphatic branching moiety at the C-8 position such as a cyclohexyloxy (**2b**, **2c**, **2g**, and **2h**) or a isopentyloxy (**2d**) group; the presence of an aryl moiety at the C-8 position, such as a phenyloxy, was also planned but unfortunately attempts to synthesize the corresponding target derivatives failed.[20] To extend the SAR, a smaller lipophilic methoxy group (**2e**) or a fluorine atom (**2f**) were also considered as C-8 substituents; the oxidation of sulphur atom to sulfone group was also realized for some derivatives (**3c**, **3e** and **3f**).

Table 1
Biological evaluation of the pyridobenzothiazole derivatives realized in this study

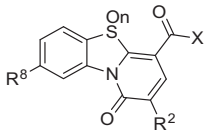

Compds	R^2	R^8	X	*n*	NS5B IC_{50}[a] (μM)	Replicon Huh 5-2	
						EC_{50}[b] (μM)	CC_{50}[b] (μM)
2a		H	OH	0	>40	53.5	>100
2b		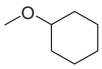	OH	0	23 ± 3[c]	>56.5	>56.5
2c		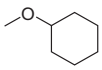	OH	0	11 ± 2[c]	>100	>100
3c		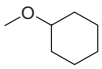	OH	2	19 ± 3[c]	55.8	>100
2d		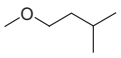	OH	0	>40	54.0	55.0
2e		OMe	OH	0	>40	51.2	51.8
3e		OMe	OH	2	>40	89.7	>100
2f		F	OH	0	>40	>100	>100
3f		F	OH	2	>40	66.0	>100
2g	COMe	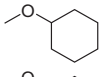	OH	0	>40	>100	>100
2h	H	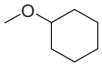	OH	0	>40	>100	>100
ATA					15 ± 3	ND[d]	ND

[a] IC_{50} = concentration of compound that inhibits enzyme activity of 50%.
[b] EC_{50} = the effective concentration required to inhibit virus induced cytopatic effect by 50% in a single experiment. CC_{50} = is the concentration required to reduce the bioreduction of MTS (3-(4,5-dimethylthiazol-2-yl)-5-(3-carboxymethoxy-phenyl)-2-(4-sulfophenyl)-2*H*-tetrazolium) in to formazan by 50%.
[c] Mean values for at least three independent experiments ± standard deviation.
[d] Not determined.

2.2. Chemistry

The synthetic procedure for the preparation of the target pyridobenzothiazole derivatives **2a**–**h**, **3c**, **3e**, and **3f** is depicted in Scheme 1. Thus, commercially available 5-hydroxybenzothiazole was reacted with cyclohexanol or isopentanol in the usual Mitsunobu reaction conditions and using ultrasound irradiation. The obtained 5-functionalized benzothiazoles **4a** and **4b**, as well as the commercially available 5-methoxy- and 5-fluoro-2-methylbenzothiazole were then demolished into the corresponding aminothiophenol intermediates **5a**, **5b**, **5c**,[21] and **5d**[21] using a mixture of aqueous 50% NaOH and ethylene glycol (1:1, v/v) at reflux. Due to the tendency of thiol groups to oxidize by air exposure to the corresponding non-reacting disulfur derivative, the crude aminothiophenol intermediates were immediately reacted with ethyl cyanoacetate to provide benzothiazole derivatives **6a**–**d**. In the same way, reaction of ethyl cyanoacetate with commercially available aminothiphenol **5e** provided benzothiazole derivative **6e**.[19]

The benzothiazole intermediates **6a**–**e** were then reacted with Vilsmeier reagent, prepared in situ by $POCl_3$ and DMF, to obtain the enamine intermediates **7a**–**e**. These were subsequently converted into pyridobenzothiazole esters **8a**–**h** by reaction with cyclohexylacetic anhydride (**8a**, **8b**), phenylacetic anhydride (**8c**–**f**), diketene (**8g**) or acetic anhydride (**8h**) in neat conditions. The hydrolysis of the ester function, in a mixture of MeOH and aqueous 4% NaOH, gave the corresponding target acids **2a**–**f** and **2h**, while a mild hydrolysis condition using 1 N LiOH and MeOH was required to achieve the target acid **2g** in order to avoid the formation of several side-products. Starting from compounds **2c**, **2e** and **2f**, the corresponding sulfone derivatives **3c**, **3e** and **3f** were obtained by oxidation with *m*-CPBA.

2.3. Biological evaluation

2.3.1. Enzymatic assay

The target compounds were tested for their ability to suppress the in vitro incorporation of [^{3}H]-UTP by recombinant HCV RNA polymerase NS5BΔC21 (genotype 1b) on a homopolymeric RNA primer/template (rA40/rU20) (Table 1). The non-nucleoside inhibitor aurintricarboxylic acid (ATA) was used as reference compound in the enzymatic assay. This compound has been shown to inhibit NS5B both in vitro and in replicon assays, through binding to the benzothiadizine allosteric pocket.[22]

Compounds **2b**, **2c**, and **3c** were able to significantly inhibit the NS5B activity with IC_{50} values ranging from 11 to 23 μM. These results highlighted that our rational design approach was successful in finding new chemotypes as NS5B inhibitors. In particular, the best anti-NS5B activity was observed for compound **2c**, functionalized with a phenyl at the C-2 and a cyclohexyloxy group at C-8 positions. The data analysis suggested that the simultaneous presence of two bulky hydrophobic groups at position C-2 and C-8 was essential to ensure anti-NS5B activity in the pyridobenzothiazole family. On the other hand, the oxidation state of the sulphur atom seemed to have no influence on the inhibitory ability, as showed by the comparable potency between sulfone derivative **3c** (IC_{50} = 19 ± 3 μM) and its parent unoxidized derivative **2c** (IC_{50} = 11 ± 2 μM).

However, these preliminary SAR remarks do not completely agree with SAR studies reported in literature for indole/benzimidazole TSI-NNIs, where a cyclohexyl group at the C-3 or N-1 position, respectively, seems essential to have high anti-NS5B activity;[23] in fact, in the pyridobenzothiazole series the presence of a cyclohexyl (**2b**) ora phenyl group (**2c** and **3c**) at the corresponding C-8 position resulted in compounds with a comparable potency.

2.3.2. Anti-HCV activity

The designed compounds were also evaluated in Huh-5-2 cells, a hepatocyte cell line stably carrying a genotype 1b subgenomic HCV replicon. The anti-viral activity (EC_{50}) was measured by the reduction of luciferase activity in the presence of increasing amount of inhibitor, while the antimetabolic effects (CC_{50}) was determined employing the MTS assay (Table 1).

Most pyridobenzothiazole derivatives proved to be not toxic with the exception of the compounds **2b**, **2d** and **2e**. A measurable anti-viral activity associated with no toxicity was obtained for the sulfone derivative **3c** (EC_{50} = 55.8 μM) and for sulphur compound **2a** (EC_{50} = 53.5 μM). However, based on the hit selection criteria (>>70% inhibition has to be observed at concentrations of compound that show no significant anti-metabolic activity) none of them could be withheld as highly potent selective inhibitor of HCV replication in the Huh-5-2 replicon system.

2.4. Binding mode analysis of hit compounds

The pyridobenzothiazole NS5B inhibitors **2b**, **2c** and **3c** were submitted to docking calculations in order to investigate their possible binding mode to the NS5B protein, and gain useful information for a further chemical optimization process.

Since the compounds arose from a scaffold-hopping approach starting from indole-based TSI-NNIs, TSI was first considered in our docking study.

However, given the above mentioned mismatch of our preliminary SAR results with the SAR studies reported in literature for different TSI-NNIs and the observation that the SAR of our compounds got somehow overlapping to the thumb site II (TSII) NNIs SAR, the possible binding modes of our pyridobenzothiazole derivatives to TSII was investigated as well. It is worth noting that beside TSI-NNIs, TSII-NNIs require the presence of two hydrophobic groups and a hydrogen bond acceptor as well.[14]

The automated docking simulations were performed using the software Glide version 5.0.[24–27]

In the absence of disclosed structural information about the **1**/NS5B interaction, the crystal structure of the HCV polymerase complexed with the indole-based TSI-NNI **9** (Fig. 2A) was used as target protein (PDB ID 2BRK)[28] to explore the first thumb pocket. This structure showed that the ligand binds to a site on the surface of the thumb domain, mainly establishing hydrophobic interaction with the surrounding NS5B residues. Indeed, the cyclohexyl group filled in a deep pocket formed by aminoacid residues of Leu-392, Ala-395, Thr-399, Ile-424, Leu-425, His-428 and Phe-429, while the phenyl ring substituent filled in a narrow pocket surrounded by Val-37, Leu-392, Ala-393, Ala-396, Leu-492 and Val-494. The indole core bridged the two groups and also contributed both in filling the pockets and in the interaction with the protein. Finally, the carboxylate moiety formed a salt bridge with the exposed Arg-503 side chain.

First of all, test docking calculations using **9** were carried out to validate the program performance. The ligand was thus extracted from the corresponding NS5B complex and then docked back into the allosteric pocket of the enzyme crystal structure. The best docking pose of **9** (XP GScore = −9.58) agreed well with its experimental binding conformation, with a root-mean square (rms) deviation value of 0.3 Å.

Later, docking of compounds **2b**, **2c** and **3c** in their anionic form (MoKa[29]-predicted p*K*a of COOH was 4.08) generated similar binding modes, which closely resembled the crystallographic position of the known inhibitor **9**. As example, Figure 2B illustrates the docked conformation of **3c** (XP GScore = −7.33), the most interesting hit of the pyridobenzothiazole series. In fact, the pyridobenzothiazole carboxylate group (CF) interacted with the Arg-503 side

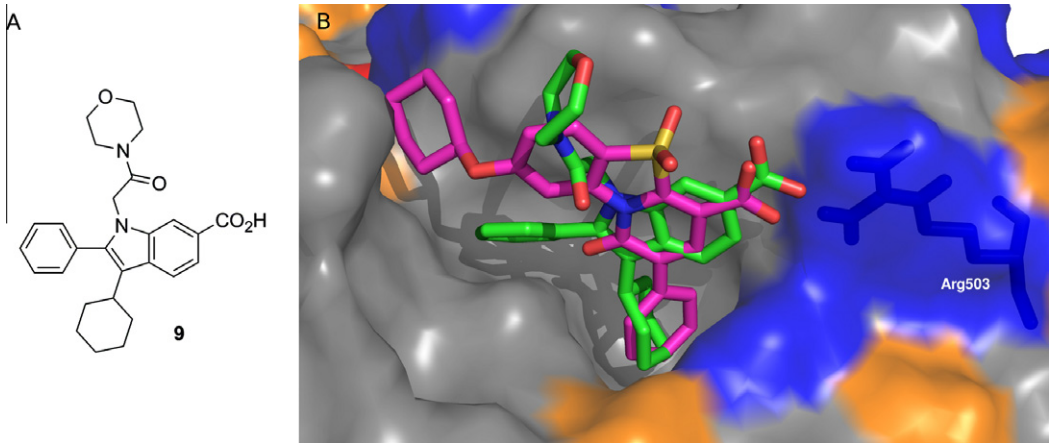

Figure 2. (A) Chemical structure of indole TSI-NNI **9**. (B) Predicted binding mode of **3c** (magenta) compared to the crystallographic position of **9** (green). Protein surface is coloured according to the aminoacid side chains: basic, blue; acidic, red; polar, orange; nonpolar, gray.

chain, while the phenyl moiety (HY2) well overlapped with the cyclohexyl ring of compound **9**. Unfortunately, a visual analysis of the docking poses also highlighted that our hit compounds were not able to properly match the hydrophobic aromatic feature HY1 of known TSI-NNIs, since the benzene ring of the pyridobenzothiazole core was about 2 Å far away from the required functionality.

On the other hand, docking studies were also performed on **1** to explore the hypothesis that the extended hydrophobic portion of our compounds might correspond to the extra hydrophobic functionality of the known inhibitor. The modelling results showed that **1** (XP GScore = −11.33) interacted with the NS5B residues of the allosteric TSI pocket in a fashion similar to **9** (Fig. 3A), with its branching moiety occupying an additional cleft mainly defined by the residues Met-36, Val-37, Cys-146, Val-147 and Leu-492.

In agreement with our design, the comparison between the docking poses of **2a**, **2b** and **3c** and the predicted binding mode of **1** highlighted that the above described additional feature occupied the same region within the TSI, being the cyclohexyl portion of our hits well overlapped with one of the branching aromatic

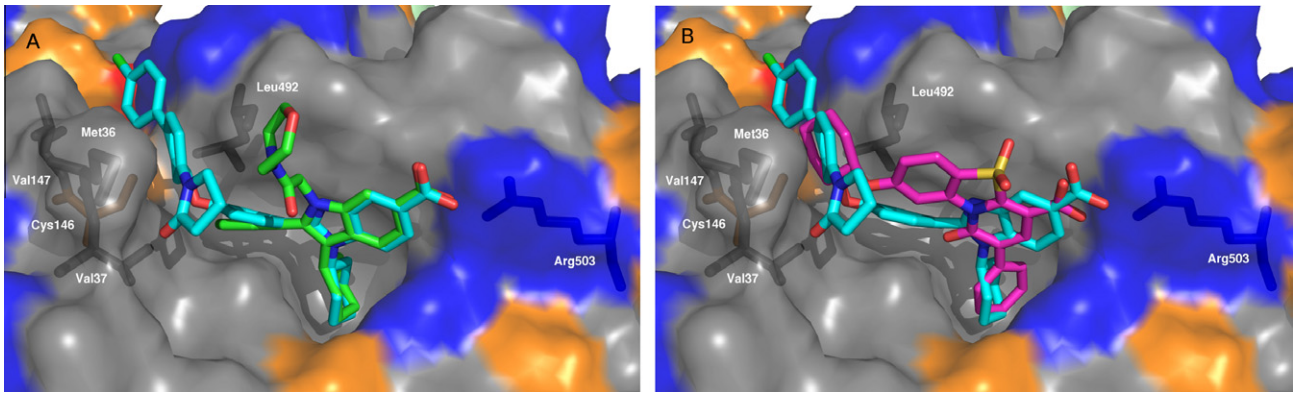

Figure 3. (A) Docking conformation of **1** (cyan) compared to the experimental position of 9 (green). (B) Docking solutions of **1** (cyan) and **3c** (magenta). Protein surface is coloured according to the aminoacid side chains: basic, blue; acidic, red; polar, orange; nonpolar, gray.

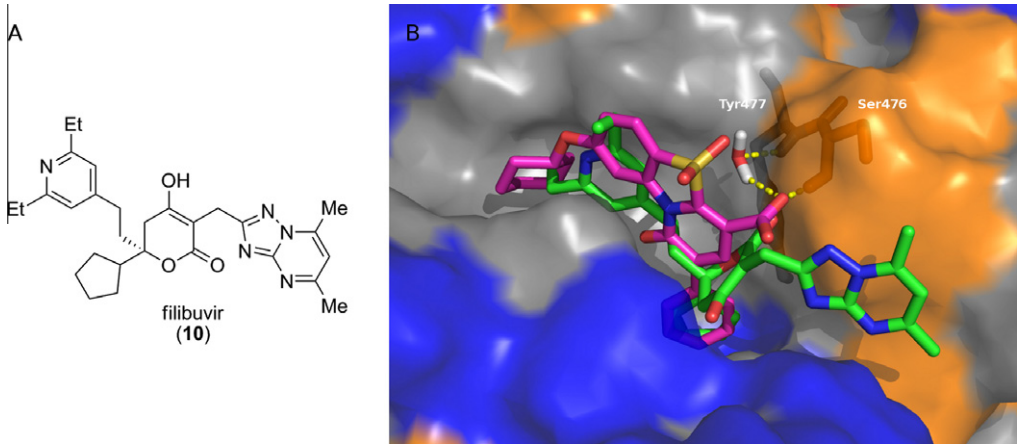

Figure 4. (A) Chemical structure of filibuvir (**10**) (B) Predicted binding mode of **3c** (magenta) compared to the crystallographic position of **10** (green). Protein surface is coloured according to the aminoacid side chains: basic, blue; acidic, red; polar, orange; nonpolar, gray.

moiety of **1**, as shown in Figure 3B for the pyridobenzothiazole derivative **3c**.

The crystal structure of NS5B polymerase in complex with PF-00868554 (**10**, filibuvir, Pfizer, Fig. 4A) (PDB code 3FRZ),[30] one of the most advanced TSII-NNIs currently in clinical trials, was instead used in the present study in order to explore the possible interactions of **2b**, **2c** and **3c** within the second thumb pocket. Structural analysis showed that the binding of the hydroxydihydropyranone derivative **10** to NS5B occurred in a predominantly hydrophobic shallow pocket at the base of the thumb domain, spacing about 35 Å from the active site. The cyclopentyl group showed key contacts with residues Leu-419, Met-423, Tyr-477, and Trp-528, whereas the two ethyl groups of the pyridine ring interacted with Leu-419, Met-423, Ile-482, Val-485, Ala-486, Leu-489, and Leu-497. A hydrogen bonding network was found between the dihydropyrone carbonyl and the donor–donor motif of the protein (backbone NH of Ser-476 and Tyr-477) through one direct hydrogen bond and one water-mediated hydrogen bond. Moreover, the enol oxygen of the inhibitor formed a second water-mediated hydrogen bond with Arg-501. Finally, the triazolopyrimidine, connected to the dihydropyrone core through a methylene linker, formed a π–π stacking interaction with His-475.

At first, we validated the ability of the docking algorithm to reproduce the co-crystallized pose of **10** within this NS5B allosteric site. This test yielded a good agreement between the in-silico docked and the crystal structure, as pointed out by the obtained rms deviation value of 0.68 Å. We next docked the three new NS5B inhibitors into the **10** binding site of NS5B. The analysis of the results highlighted that, analogously to what observed in the docking studies on TSI, **2b**, **2c** and **3c** generated reasonable binding modes, similar to **10**, within the second thumb pocket. For instance, Figure 4B shows the obtained docking pose for compound **3c** (XP GScore value = −7.43). The pyridobenzothiazole carboxylate group (CF) formed the same hydrogen bonding network with Ser-476 and Tyr-477 as observed for the dihydropyrone carbonyl group of **10**. The phenyl moiety (HY2) well overlapped with the cyclopentyl ring of the co-crystallized inhibitor, whereas the aromatic feature HY1 and the extended hydrophobic portion of our compounds showed the same hydrophobic interactions observed for the two ethyl groups of **10**.

Given that, as mentioned above, the two allosteric thumb sites have similar requirements for inhibitor binding, it was not surprising to observe that our compounds could potentially exhibit similar affinity towards either TSI or TSII of NS5B. A thorough in-silico analysis of the docking models of the pyridobenzothiazole derivatives within both pockets could serve as a guide for future design and development of more potent NS5B inhibitors.

2.5. Mechanism of inhibition study

Given the initial design principle and the molecular modeling results, the mechanism of inhibition of our compounds could be due to the perturbation of the dynamic properties of the thumb domain.[31] For example, inhibitor binding could interfere with the thumb β-loop motion, which has been proposed to interact with the RNA template during elongation. In addition, residues in the thumb-palm junction might contact the nascent primer strand. Finally, the lysine-arginine rich domain of the thumb has been proposed to have a role in NS5B-RNA contacts. In order to define the mechanism of inhibition, the potency of compounds **2b**, **2c** and **3c** was evaluated in the in vitro assay, in the presence of varying concentrations of either UTP or the RNA primer/template. No effect of UTP concentration was observed on the inhibition (data not shown). On the contrary, the potency of all compounds was decreased by increasing the RNA template/primer concentration (Fig. 5). These results suggest that the allosteric effects caused by our compounds interfere with the interaction between NS5B and the RNA template.

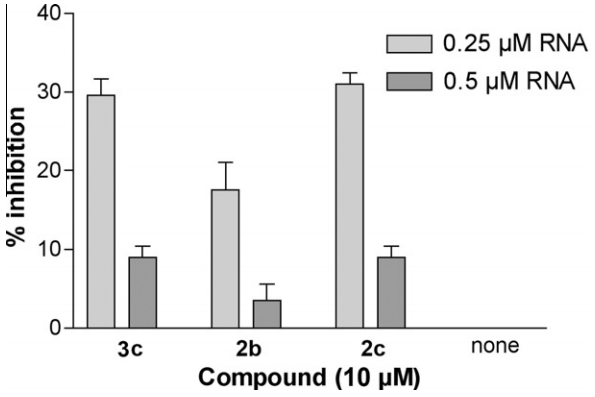

Figure 5. Dependence of the inhibitory activity of compounds **2b**, **2c** and **3c** from the RNA concentration. Inhibition of NS5B incorporation of UTP on the (rA)40/(rU)20, primer template was tested in the presence of a fixed subsaturating (i.e., $<IC_{50}$) dose of inhibitor and two increasing doses of RNA template. Values are expressed as % of inhibition with respect to control reactions in the absence of the compounds. Plotted values are means of three independent determinations. Error bars are ±S.D.

3. Conclusions

The rational approach employed for the design of novel pyridobenzothiazole-based TSI-NNIs led to the identification of new hit compounds (**2b**, **2c** and **3c**) showing interesting inhibitory activities in the enzymatic assay. Unfortunately, their cell-based anti-HCV activities do not fully reflect the observed NS5B enzymatic inhibition; it may be supposed that the lack of remarkable cellular activity could be due to permeability issue. Molecular docking results suggested that the new NS5B inhibitors could bind either TSI or TSII, despite the difference in scaffold and substitutions. Biochemical studies provided further clues about a possible mechanism of allosteric inhibition, showing that the pyridobenzothiazole derivatives are non-competitive inhibitors with respect to the ribonucleotide substrate and competitive inhibitors with respect to the RNA template. Using the information mined from this study and with the aim to improve both anti-NS5B and cell-based anti-HCV activities, the design and synthesis of novel derivatives will be the next step of this drug discovery project. Afterwards, once stronger binders will be obtained, our efforts will be dedicated to experimentally provide full proof of the exact binding site for the pyridobenzothiazole derivatives.

4. Experimental section

4.1. Synthesis and compound characterization

All starting materials were commercially available, unless otherwise indicated. Reagents and solvents were purchased from common commercial suppliers and were used as such. Organic solutions were dried over anhydrous Na_2SO_4 and concentrated with a rotary evaporator at low pressure. All reactions were routinely checked by thin-layer chromatography (TLC) on silica gel 60F254 (Merck) and visualized by using UV or iodine. Column chromatography separations were carried out on Merck silica gel 60 (mesh 70–230), flash chromatography on Merck silica gel 60 (mesh 230–400). Ultrasound reactions were conducted using Decon ultrasonic LTD machinery. Melting points were determined in capillary tubes (Büchi Electrotermal model 9100) and are uncorrected. Yields were of purified products and were not optimized.

^{1}H NMR spectra were recorded at 200 or 400 MHz (Bruker Avance DRX-200 or 400, respectively) while ^{13}C NMR spectra were recorded at 100 MHz (Bruker Avance DRX-400). Chemical shifts are given in ppm (δ) relative to TMS. Spectra were acquired at 298 K. Data processing was performed with standard Bruker software XwinNMR and the spectral data are consistent with the assigned structures. HRMS experiments were performed in the positive ion mode using electron spray ionization (ESI) source; the LC–MS machine consist of an HPLC Agilent 1290 Infinity System equipped with a MS detector Agilent 6540UHD Accurate Mass Q-TOF. Elemental analyses were performed on a Fisons elemental analyzer, model EA1108CHN, and data for C, H, and N are within 0.4% of the theoretical values.

4.1.1. 5-(Cyclohexyloxy)-2-methyl-1,3-benzothiazole (4a)

Diethyl azodicarboxylate (DEAD) (5.4 mL, 27.24 mmol) was added dropwise, over 30 min, to a solution of 2-methyl-1,3-benzothiazol-5-ol (3.00 g, 18.16 mmol), cyclohexanol (2.8 mL, 27.24 mmol), PPh_3 (7.15 g, 27.24 mmol) and Et_3N (2.65 mL, 19.07 mmol) in dry THF (60 mL), placed in a ultrasound bath. The mixture was sonicated for 72 h and then evaporated to dryness. The residue was purified by column chromatography, eluting with CH_2Cl_2, to give **4a** (3.00 g, 67%) as brown solid; ^{1}H NMR (200 MHz, DMSO-d_6) δ 1.20–1.50 (m, 6H, cycloxeyl CH_2), 1.60–1.70 and 1.85–1.95 (each m, 2H, cyclohexyl CH_2), 2.70 (s, 3H, CH_3), 4.25–4.35 (m, 1H, cyclohexyl CH), 6.95 (dd, J = 2.3 and 8.8 Hz, 1H, H-6), 7.40 (d, J = 2.3 Hz, 1H, H-4), 7.80 (d, J = 8.8 Hz, 1H, H-7). HRMS (ESI) calcd for $C_{14}H_{18}NOS$ $(M+H)^+$ 248.11091, found 248.10865.

4.1.1.1. 5-(Isopentyloxy)-2-methyl-1,3-benzothiazole (4b). The title compound was obtained in manner similar to that used to synthesize compound **4a**, replacing cyclohexanol with isopenatanol: brown oil, 89% yield; ^{1}H NMR (200 MHz, DMSO-d_6) δ 0.80 (d, J = 6.4 Hz, 6H, isopentyloxy CH_3), 1.50 (q, J = 6.6 Hz, 2H, isopentyloxy CH_2), 1.60–1.70 (m, 1H, isopentyloxy CH), 2.75 (s, 3H, CH_3), 3.90 (t, J = 6.6 Hz, 2H, isopentyloxy CH_2), 6.90 (dd, J = 2.3 and 8.8 Hz, 1H, H-6), 7.30 (d, J = 2.3 Hz, 1H, H-4), 7.73 (d, J = 8.8 Hz, 1H, H-7). HRMS (ESI) calcd for $C_{13}H_{18}NOS$ $(M+H)^+$ 236.11091, found 236.10860.

4.1.2. Ethyl [5-(cyclohexyloxy)-1,3-benzothiazol-2-yl]acetate (6a)

A solution of compound **4a** (3.73 g, 15.10 mmol) in a mixture of 1:1 v/v aqueous 50% NaOH and ethylene glycol (45 mL) was refluxed under N_2 flux until the starting material disappeared. The mixture was then poured into ice-water, acidified to pH ~3 with 2 N HCl and extracted several times with CH_2Cl_2. The combined organic layers were dried and evaporated to dryness to give crude aminothiophenol derivative **5a** as yellow oil (2.1 g) which was immediately reacted with ethyl cyanoacetate (2 mL) at 120 °C under stirring and N_2 flux. After 15 h, the mixture was cooled and then treated with Et_2O (30 mL). After washing with diluted HCl and then with diluted NaOH, the organic solution was dried and evaporated to dryness. The residue was purified by column chromatography, eluting with cyclohexane/EtOAc (9:1), to give **6a** (1.05 g, 22% two-step overall yield) as yellowish solid; ^{1}H NMR (200 MHz, $CDCl_3$) δ 1.20–1.60 (m, 9H, cyclohexyl CH_2 and OCH_2CH_3), 1.60–1.70 and 1.90–2.00 (each m, 2H, cyclohexyl CH_2), 4.15–4.40 (m, 5H, cyclohexyl CH, CH_2 and OCH_2CH_3), 7.05 (dd, J = 2.5 and 8.7 Hz, 1H, H-6), 7.50 (d, J = 2.5 Hz, 1H, H-4), 7.65 (d, J = 8.7 Hz, 1H, H-7). HRMS (ESI) calcd for $C_{17}H_{22}NO_3S$ $(M+H)^+$ 320.13204, found 320.13287.

4.1.2.1. Ethyl [5-(3-isopentyloxy)-1,3-benzothiazol-2-yl]acetate (6b). The title compound was obtained in manner similar to that used to synthesize compound **6a**, starting from benzothiazole **4b**: pale yellow oil, 14% two-step overall yield; ^{1}H NMR (200 MHz, $CDCl_3$) δ 0.90 (d, J = 6.4 Hz, 6H, isopentyl CH_3), 1.20 (t, J = 7.1 Hz, 3H, OCH_2CH_3), 1.40–1.80 (m, 3H, isopentyl CH and isopentyl CH_2), 3.90–4.25 (m, 6H, isopentyl CH_2, CH_2 and OCH_2CH_3), 6.90 (dd, J = 2.3 and 8.9 Hz, 1H, H-6), 7.35 (d, J = 2.3 Hz, 1H, H-4), 7.55 (d, J = 8.9 Hz, 1H, H-7). HRMS (ESI) calcd for $C_{16}H_{22}NO_3S$ $(M+H)^+$ 308.13204, found 303.13267.

4.1.2.2. Ethyl (5-methoxy-1,3-benzothiazol-2-yl)acetate (6c). The title compound was obtained in manner similar to that used to synthesize compound **6a**, starting from commercially available 5-methoxy-2-methyl-1,3-benzothiazole: brown oil, 93% two-step overall yield; ^{1}H NMR (200 MHz, DMSO-d_6) δ 1.10 (t, J = 7.1 Hz, 3H, OCH_2CH_3), 3.70 (s, 3H, OCH_3), 4.05 (q, J = 7.1 Hz, 2H, OCH_2CH_3), 4.20 (s, 2H, CH_2), 6.95 (dd, J = 2.5 and 8.8 Hz, 1H, H-6), 7.40 (d, J = 2.5 Hz, 1H, H-4), 7.80 (d, J = 8.8 Hz, 1H, H-7). HRMS (ESI) calcd for $C_{12}H_{13}NO_3S$ $(M+H)^+$ 252.06944, found 252.07005.

4.1.2.3. Ethyl (5-fluoro-1,3-benzothiazol-2-yl)acetate (6d). The title compound was obtained in manner similar to that used to synthesize compound **6a**, starting from commercially available 5-fluoro-2-methyl-1,3-benzothiazole: yellowish solid, 74% two-step overall yield; ^{1}H NMR (200 MHz, DMSO-d_6) δ 1.10 (t, J = 7.1 Hz, 3H, OCH_2CH_3), 4.00 (q, J = 7.1 Hz, 2H, OCH_2CH_3), 4.25 (s, 2H, CH_2), 7.20 (dt, J = 2.5 and 8.9 Hz, 1H, H-6), 7.70 (dd, J = 2.5 and 10.0 Hz, 1H, H-4), 8.00 (dd, J = 5.4 and 8.9 Hz, 1H, H-7). HRMS (ESI) calcd for $C_{11}H_{10}FNO_2S$ $(M+H)^+$ 240.04946, found 240.04980.

4.1.3. Ethyl 2-[5-(cyclohexyloxy)-1,3-benzothiazol-2-yl]-3-(dimethylamino)acrylate (7a)

A mixture of compound **6a** (2.24 g, 7.01 mmol) and Vilsmeier reagent, prepared in situ from $POCl_3$ (1.30 mL, 14.02 mmol) and DMF (1.40 mL, 21.03 mmol), was heated at 90 °C under stirring for 2 h. After cooling, the mixture was treated with ice-water, basified to pH ~8 with solid K_2CO_3 and extracted several times with $CHCl_3$. The combined organic layers were dried and evaporated to dryness giving a residue which was purified by column chromatography, eluting with cyclohexan/EtOAc (6:4), to give **7a** (2.17 g, 83%) as yellowish solid; ^{1}H NMR (200 MHz, $CDCl_3$) δ 1.50–1.70 (m, 9H, cyclohexyl CH_2 and OCH_2CH_3), 1.80–1.95 (m, 4H, cyclohexyl CH_2), 3.05 and 3.35 (each s, 3H, NCH_3), 4.10–4.25 (m, 3H, cyclohexyl CH and OCH_2CH_3), 6.90 (dd, J = 2.3 and 8.8 Hz, 1H, H-6), 7.50 (d, J = 2.3 Hz, 1H, H-4), 7.65 (d, J = 8.8 Hz, 1H, H-7), 9.05 (s, 1H, CH). HRMS (ESI) calcd for $C_{20}H_{27}N_2O_3S$ $(M+H)^+$ 375.17424, found 375.17198.

4.1.3.1. Ethyl 3-(dimethylamino)-2-[5-(3-isopentyloxy)-1,3-benzothiazol-2-yl]acrylate (7b). The title compound was obtained in manner similar to that used to synthesize compound **7a**, starting from derivative **6b**: yellowish gum, 50% yield; ^{1}H NMR (200 MHz, $CDCl_3$) δ 0.98 (d, J = 6.5 Hz, 6H, isopentyl CH_3), 1.25 (t, J = 7.0 Hz, 3H, OCH_2CH_3), 1.40–1.80 (m, 3H, isopentyl CH and isopentyl CH_2), 3.25 (bs, 6H, NCH_3), 4.11 (t, J = 7.0 Hz, 2H, isopentyl CH_2), 4.30 (q, J = 7.0 Hz, 2H, OCH_2CH_3), 6.98 (dd, J = 2.3 and 8.8 Hz, 1H, H-6), 7.55 (d, J = 2.5 Hz, 1H, H-4), 7.65 (d, J = 8.8 Hz, 1H, H-7), 8.40 (s, 1H, CH). HRMS (ESI) calcd for $C_{19}H_{27}N_2O_3S$ $(M+H)^+$ 362.17424, found 362.17194.

4.1.3.2. Ethyl 3-(dimethylamino)-2-(5-methoxy-1,3-benzothiazol-2-yl)acrylate (7c). The title compound was obtained in manner similar to that used to synthesize compound **7a**, starting from derivative **6c**: yellowish solid, 88% yield; ^{1}H NMR (200 MHz, DMSO-d_6) δ 1.10 (t, J = 7.1 Hz, 3H, OCH_2CH_3), 3.05 (bs, 6H, NCH_3), 3.70 (s, 3H, OCH_3), 4.10 (q, J = 7.1 Hz, 2H, OCH_2CH_3), 6.85 (dd, J = 2.2 and 8.8 Hz, 1H, H-6), 7.20 (d, J = 2.2 Hz, 1H, H-4), 7.70 (d, J = 8.8 Hz, 1H, H-7), 8.10 (s, 1H, CH). HRMS (ESI) calcd for $C_{15}H_{19}N_2O_3S$ $(M+H)^+$ 307.11164, found 307.10931.

4.1.3.3. Ethyl 2-(5-fluoro-1,3-benzothiazol-2-yl)-3-(dimethylamino)acrylate (7d). The title compound was obtained in manner similar to that used to synthesize compound **7a**, starting from derivative **6d**: yellowish solid, 78% yield; ^{1}H NMR (200 MHz, $CDCl_3$) δ 1.10 (t, J = 7.1 Hz, 3H, OCH_2CH_3), 2.95 (bs, 6H, NCH_3), 4.05 (q, J = 7.1 Hz, 2H, OCH_2CH_3), 6.95–7.05 (dt, J = 2.5 and 8.8 Hz, 1H, H-6), 7.50 (dd, J = 2.5 and 10.2 Hz, 1H, H-4), 7.80 (dd, J = 5.5 and 8.8 Hz, 1H, H-7), 7.95 (s, 1H, CH). HRMS (ESI) calcd for $C_{14}H_{16}FN_2O_2S$ $(M+H)^+$ 295.09166, found 295.09194.

4.1.4. Ethyl 8-(cyclohexyloxy)-1-oxo-2-phenyl-1*H*-pyrido[2,1-*b*]benzothiazole-4-carboxylate (8c)

A mixture of acrylate **7a** (0.10 g, 0.27 mmol) and phenylacetic anhydride (0.13 g, 0.53 mmol), was heated at 100 °C, under stirring, for 5 h. After cooling, the residue was triturated with Et_2O to give compound **8c** (0.10 g, 83%) as yellow solid; ^{1}H NMR (200 MHz, DMSO-d_6) δ 1.25–1.60 (m, 9H, cyclohexyl CH_2 and OCH_2CH_3), 1.65–1.85 and 1.90–2.00 (each m, 2H, cyclohexyl CH_2), 4.20–4.50 (m, 3H, cyclohexyl CH and OCH_2CH_3), 7.20 (dd, J = 2.4 and 8.7 Hz, 1H, H-7), 7.30–7.50 (m, 3H, Ar-H), 7.70 (d, J = 8.7 Hz, 1H, H-6), 7.60–7.75 (m, 2H, Ar-H), 8.00 (s, 1H, H-3), 8.75 (d, J = 2.4 Hz, 1H, H-9). HRMS (ESI) calcd for $C_{26}H_{26}NO_4S$ $(M+H)^+$ 448.15826, found 448.16045.

4.1.4.1. Ethyl 2-cyclohexyl-8-(cyclohexyloxy)-1-oxo-1*H*-pyrido[2,1-*b*][1,3]benzothiazole-4-carboxylate (8b). The title compound was prepared according to the procedure used for compound **8c** starting from acrylate **7a** and replacing phenylacetic anhydride with cyclohexylacetic anhydride. The residue was purified by flash column chromatography, eluting with cyclohexane/EtOAc (95:5), to give **8b** (40%) as white solid; ^{1}H NMR (200 MHz, DMSO-d_6) δ 1.10–1.60 (m, 15 H, cyclohexyl CH_2 and OCH_2CH_3), 1.70–2.00 (m, 8H, cyclohexyl CH_2), 2.75–2.80 (m, 1H, cyclohexyl CH), 4.30–4.45 (m, 3H, cyclohexyl CH and OCH_2CH_3), 7.20 (dd, J = 2.4 and 8.8 Hz, 1H, H-7), 7.75 (s, 1H, H-3), 7.90 (d, J = 8.8 Hz, 1H, H-6), 8.80 (d, J = 2.4 Hz, 1H, H-9). HRMS (ESI) calcd for $C_{26}H_{32}NO_4S$ $(M+H)^+$ 454.20521, found 454.20294.

4.1.4.2. Ethyl 2-cyclohexyl-1-oxo-1*H*-pyrido[2,1-*b*][1,3]benzothiazole-4-carboxylate (8a). The title compound was prepared according to the procedure used for compound **8c** starting from acrylate **7e** and replacing phenylacetic anhydride with cyclohexylacetic anhydride. The residue was purified by flash column chromatography, eluting with cyclohexane/EtOAc (95:5), to give **8a** (37%) as yellowish solid; ^{1}H NMR (200 MHz, $CDCl_3$) δ 1.15–1.65 (m, 9 H, cyclohexyl CH_2 and OCH_2CH_3), 1.75–2.10 (m, 4H, cyclohexyl CH_2), 2.35–2.45 (m, 1H, cyclohexyl CH), 4.30 (q, J = 7.0 Hz, 2H, OCH_2CH_3), 7.45–7.55 (m, 2H, H-7 and H-8), 7.60–7.80 (m. 1H, H-6), 7.90 (s, 1H, H-3), 9.30–9.40 (m, 1H, H-9). HRMS (ESI) calcd for $C_{20}H_{22}NO_3S$ $(M+H)^+$ 356.13204, found 356.12972.

4.1.4.3. Ethyl 8-(isopentyloxy)-1-oxo-2-phenyl-1*H*-pyrido[2,1-*b*][1,3]benzothiazole-4-carboxylate (8d). The title compound was prepared according to the procedure used for compound **8c** starting from compound **7b**: white solid, 30% yield; ^{1}H NMR (200 MHz, DMSO-d_6) δ 0.90 (d, 6H, J = 6.5 Hz, isopentyl CH_3), 1.35 (t, 3H, J = 7.0 Hz, OCH_2CH_3), 1.60–1.85 (m, 3H, isopentyl CH and isopentyl CH_2), 4.10 (t, 2H, J = 6.5 Hz, isopentyl CH_2), 4.35 (q, 2H, J = 7.0 Hz, OCH_2CH_3), 7.25 (dd, 1H, J = 2.4 and 8.8 Hz, H-7), 7.30–7.50 (m, 3H, Ar-H), 7.70–7.75 (m, 2H, Ar-H), 8.00 (d, 1H, J = 8.8 Hz, H-6), 8.10 (s, 1H, H-3), 8.85 (d, 1H, J = 2.4 Hz, H-9). HRMS (ESI) calcd for $C_{25}H_{26}NO_4S$ $(M+H)^+$ 436.15826, found 436.15590.

4.1.4.4. Ethyl 8-methoxy-1-oxo-2-phenyl-1*H*-pirido[2,1-*b*][1,3]benzothiazole-4-carboxylate (8e). The title compound was prepared according to the procedure used for compound **8c** starting from compound **7c**: white solid, 84% yield; ^{1}H NMR (200 MHz, DMSO-d_6) δ 1.22 (t, J = 7.1 Hz, 3H, OCH_2CH_3), 3.75 (s, 3H, OCH_3), 4.25 (q, J = 7.1 Hz, 2H, OCH_2CH_3), 7.10 (dd, J = 2.5 and 8.8 Hz, 1H, H-7), 7.35–7.40 (m, 3H, Ar-H), 7.55–7.60 (m, 2H, Ar-H), 7.90 (d, J = 8.8 Hz, 1H, H-6), 7.95 (s, 1H, H-3), 8.70 (d, J = 2.5 Hz, 1H, H-9). HRMS (ESI) calcd for $C_{21}H_{18}NO_4S$ $(M+H)^+$ 380.09566, found 380.09572.

4.1.4.5. Ethyl 8-fluoro-1-oxo-2-phenyl-1*H*-pyrido[2,1-*b*]benzothiazole-4-carboxylate (8f). The title compound was prepared according to the procedure used for compound **8c** starting from compound **7d**: yellow solid, 68% yield; ^{1}H NMR (200 MHz, DMSO-d_6) δ 1.25 (t, J = 6.9 Hz, 3H, OCH_2CH_3), 4.25 (q, J = 6.9 Hz, 2H, OCH_2CH_3), 7.20–7.45 (m, 4H, H-7 and Ar-H), 7.55–7.65 (m, 2H, Ar-H), 7.95–8.15 (m, 2H, H-3 and H-6), 8.80–8.90 (m, 1H, H-9). HRMS (ESI) calcd for $C_{20}H_{15}FNO_3S$ $(M+H)^+$ 368.07567, found 368.07792.

4.1.4.6. Ethyl 2-acetyl-8-(cyclohexyloxy)-1-oxo-1*H*-pyrido[2,1-*b*] [1,3]benzothiazole-4-carboxylate (8g). The title compound was prepared according to the procedure used for compound **8c** starting from compound **7a** and replacing phenylacetic anhydride with diketene: yellow solid, 69% yield; ^{1}H NMR (200 MHz, DMSO-d_6) δ 1.10–1.45 (m, 9H, cyclohexyl CH_2 andOCH_2CH_3), 1.55–1.70 and 1.75–1.95 (each m, 2H, cyclohexyl CH_2), 2.55 (s, 3H, $COCH_3$), 4.10–4.45 (m, 3H, cyclohexyl CH and OCH_2CH_3), 7.20 (dd, J = 2.8 and 8.7 Hz, 1H, H-7), 7.95 (d, J = 8.7 Hz, 1H, H-6), 8.45 (s, 1H, H-3), 8.70 (d, J = 2.8 Hz, 1H, H-9). HRMS (ESI) calcd for $C_{22}H_{23}NO_5S$ $(M+H)^+$ 414.13752, found 414.13642.

4.1.4.7. Ethyl 8-(cyclohexyloxy)-1-oxo-1*H*-pyrido[2,1-*b*][1,3]benzothiazole-4-carboxylate (8h). The title compound was prepared according to the procedure used for compound **8c** starting from compound **7a** and replacing phenylacetic anhydride with acetic anhydride: orange solid, 53% yield; ^{1}H NMR (200 MHz, DMSO-d_6) δ 1.10–1.50 (m, 9H, cyclohexyl CH_2 and OCH_2CH_3), 1.50–1.70 and 1.75–1.95 (each m, 2H, cyclohexyl CH_2), 4.15–4.30 (m, 3H, cyclohexyl CH and OCH_2CH_3), 6.30 (d, J = 9.5 Hz, 1H, H-2), 7.15 (dd, J = 2.4 and 8.8 Hz, 1H, H-7), 7.85–8.00 (m, 2H, H-3 and H-6), 8.70 (d, J = 2.4 Hz, 1H, H-9). HRMS (ESI) calcd for $C_{20}H_{21}NO_4S$ $(M+H)^+$ 372.12696, found 372.12468.

4.1.5. 8-(Cyclohexyloxy)-1-oxo-2-phenyl-1*H*-pyrido[2,1-*b*][1,3]benzothiazole-4-carboxylic acid (2c)

A mixture of compound **8c** (0.29 g, 0.65 mmol) in aqueous 10% NaOH (7.25 mL) and MeOH (29 mL) was heated at 75 °C for 2 h. After cooling, the mixture was concentrated, poured in ice/H_2O, acidified to pH ~3 with 2 N HCl and extracted with CH_2Cl_2. The combined organic layers were dried and evaporated to dryness giving a residue which was triturated with Et_2O and collected by filtration. Compound **2c** (0.21 g, 78%) was obtained as pale yellow solid: mp 275–278 °C (decompose); ^{1}H NMR (400 MHz, DMSO-d_6) δ 1.22–1.55 (m, 6H, cyclohexyl CH_2), 1.65–1.75 and 1.90–2.00 (each m, 2H, cyclohexyl CH_2), 4.30–4.45 (m, 1H, cyclohexyl CH), 7.20 (dd, J = 2.2 and 8.7 Hz, 1H, H-7), 7.30–7.35 (m, 1H, Ar-H), 7.40–7.50 (m, 2H, Ar-H), 7.67–7.75 (m, 2H, Ar-H), 7.95 (d, J = 8.7 Hz, 1H, H-6), 8.10 (s, 1H, H-3), 8.80 (d, J = 2.2 Hz, 1H, H-9), 12.70 (bs, 1H, CO_2H). ^{13}C NMR (400 MHz, DMSO-d_6): δ 25.46, 25.51, 31.54, 75.70, 103.48, 107.35, 116.62, 119.96, 122.62, 123.34, 127.86, 128.55, 129.09, 136.01, 136.58, 139.22, 153.63, 156.52, 161.46, 166.36. HRMS (ESI) calcd for $C_{24}H_{22}NO_4S$ $(M+H)^+$ 420.12696, found 420.12683. Anal. calcd for $C_{24}H_{21}NO_4S$: C, 68.72; H, 5.05; N, 3.34. Found: C, 68.82; H, 5.15; N, 3.14.

4.1.5.1. 2-Cyclohexyl-1-oxo-1*H*-pyrido[2,1-*b*][1,3]benzothiazole-4-carboxylic acid (2a). The title compound was prepared according to the procedure used for compound **2c** starting from compound **8a**. Compound **2a** (30%) was obtained as brown solid: mp 266–268 °C; ^{1}H NMR (400 MHz, DMSO-d_6) δ 1.10–1.50 (m, 6H, CH_2cyclohexyl), 1.70–1.90 (m, 4H, cyclohexyl CH_2), 2.79–2.90 (m, 1H, cyclohexyl CH), 7.50–7.60 (m, 2H, H-7 and H-8), 7.95 (s, 1H, H-3), 8.00–8.10 (m, 1H, H-6), 9.15–9.20 (m, 1H, H-9), 12.70 (bs, 1H, CO_2H). ^{13}C NMR (DMSO-d_6) δ 26.21, 26.85, 32.31, 37.33, 102.87, 119.75, 122.88, 126.82, 127.23, 128.63, 129.93, 132.23, 137.85, 150.57, 162.73, 166.57. HRMS (ESI) calcd for $C_{18}H_{18}NO_3S$ $(M+H)^+$ 328.10074, found 328.10059. Anal. calcd for $C_{18}H_{17}NO_3S$: C, 66.03; H, 5.23; N, 4.28. Found: C, 66.06; H, 5.26; N, 4.11.

4.1.5.2. 2-Cyclohexyl-8-(cyclohexyloxy)-1-oxo-1*H*-pyrido[2,1-*b*][1,3]benzothiazole-4-carboxylic acid (2b). The title compound was prepared according to the procedure used for compound **2c** starting from compound **8b**. Compound **2b** (85%) was obtained as white solid: mp 307–310 °C (decompose); ^{1}H NMR (400 MHz, DMSO-d_6) δ 1.10–1.50 (m, 12H, cyclohexyl CH_2), 1.70–1.90 (m, 8H, cyclohexyl CH_2), 2.75–2.90 (m, 1H, cyclohexyl CH), 4.30–4.50 (m, 1H, cyclohexyl CH), 7.10 (dd, J = 2.2 and 8.7 Hz, 1H, H-7), 7.75 (d, J = 8.7 Hz, 1H, H-6), 7.85 (s, 1H, H-3), 8.90 (d, J = 2.2 Hz, 1H, H-9). ^{13}C NMR (400 MHz, DMSO-d_6) δ 23.50, 25.57, 26.36, 27.00, 31.66, 32.76, 37.11, 75.66, 107.48, 111.35, 115.84, 122.27, 122.52, 128.34, 134.11, 139.41, 147.63, 155.67, 162.64, 167.52. HRMS (ESI) calcd for $C_{24}H_{28}NO_4S$ $(M+H)^+$ 426.17391, found 426.17393. Anal. calcd for $C_{24}H_{27}NO_4S$: C, 67.74; H, 6.40; N, 3.29. Found C, 67.89; H, 6.55; N, 2.99.

4.1.5.3. 2-Acetyl-8-(cyclohexyloxy)-1-oxo-1*H*-pyrido[2,1-*b*][1,3]benzothiazole-4-carboxylic acid (2g). $LiOH{\cdot}2H_2O$ (0.04 g, 0.90 mmol) was added to a solution of compound **8g** (0.12 g, 0.30 mmol) in a mixture of dioxane/H_2O (4 mL, 3:1). The reaction mixture was stirred at 40 °C for 4 days, then poured into water, acidified with AcOH and extracted several times with EtOAc. The combined organic layers were dried and evaporated to dryness giving a residue which was triturated with Et_2O and filtered. Compound **2g** (0.08 g, 88%) was obtained as pale orange solid: mp 299–300 °C (decompose); ^{1}H NMR (400 MHz, DMSO-d_6) δ 1.10–1.60 (m, 6H, cyclohexyl CH_2), 1.65–1.80 and 1.85–2.10 (m, each 2H, cyclohexyl CH_2), 2.70 (s, 3H, CH_3), 4.40–4.55 (m, 1H, cyclohexyl CH), 7.30 (dd, J = 2.2 and 8.8 Hz, 1H, H-7), 8.05 (d, J = 8.8 Hz, 1H, H-6), 8.60 (s, 1H, H-3), 8.85 (d, J = 2.2 Hz, 1H, H-9), 13.50 (bs, 1H, CO_2H). ^{13}C NMR (DMSO-d_6) δ 23.41, 25.51, 31.33, 31.50, 75.75, 107.55, 116.94, 118.44, 120.46, 123.75, 139.45, 140.42, 156.92, 159.38, 161.51, 166.11, 195.56. HRMS (ESI) calcd for $C_{20}H_{20}NO_5S$ $(M+H)^+$ 386.10622, found 386.10578. Anal. calcd for $C_{20}H_{19}NO_5S$: C, 62.32; H, 4.97; N, 3.63. Found: C, 62.12; H, 4.57; N, 4.03.

4.1.5.4. 8-(Cyclohexyloxy)-1-oxo-1*H*-pyrido[2,1-*b*][1,3]benzothiazole-4-carboxylic acid (2h). The title compound was prepared according to the procedure used for compound **2c** starting from compound **8h**. Compound **2h** (75%) was obtained as pale yellow solid: mp 297–298 °C; ^{1}H NMR (400 MHz, DMSO-d_6) 1.30–1.55 (m, 6H, cyclohexyl CH_2), 1.65–1.75 and 1.90–2.00 (each m, 2H, cyclohexyl CH_2), 4.30–4.40 (m, 1H, cyclohexyl CH), 6.25 (d, J = 9.4 Hz, 1H, H-2), 7.10 (dd, J = 2.4 and 8.8 Hz, 1H, H-7), 7.85 (d, J = 8.8 Hz, 1H, H-6), 8.05 (d, J = 9.4 Hz, 1H, H-3), 8.80 (d, J = 2.4 Hz, 1H, H-9). ^{13}C NMR (DMSO-d_6) δ 23.53, 25.51, 31.58, 75.79, 107.23, 111.35, 111.97, 116.32, 119.76, 123.31, 138.27, 138.98, 154.89, 156.53, 162.38, 166.33. HRMS (ESI) calcd for $C_{18}H_{18}NO_4S$ $(M+H)^+$ 344.09566, found 344.09540. Anal. calcd for $C_{18}H_{17}NO_4S$: C, 62.96; H, 4.99; N, 4.08. Found: C, 62.74; H, 4.71; N, 4.48.

4.1.5.5. 8-(Isopentyloxy)-1-oxo-2-phenyl-1*H*-pyrido[2,1-*b*][1,3]benzothiazole-4-carboxylic acid (2d). The title compound was prepared according to the procedure used for compound **2c** starting from compound **8d**. Compound **2d** (40%) was obtained as white solid: mp 268–270 °C; ^{1}H NMR (400 HHz, DMSO-d_6) δ 0.95 (d, J = 6.6 Hz, 6H, isopentyl CH_3), 1.65 (q, J = 6.6 Hz, 2H, isopentyl CH_2), 1.75–1.85 (m, 1H, isopentyl CH), 4.05 (t, J = 6.6 Hz, 2H, isopentyl CH_2), 7.15 (dd, J = 2.3 and 8.8 Hz, 1H, H-7), 7.35–7.40 (m, 1H, Ar-H), 7.40–7.45 (m, 2H, Ar-H), 7.70–7.75 (m, 2H, Ar-H), 7.90 (d, J = 8.8 Hz, 1H, H-6), 8.10 (s, 1H, H-3), 8.80 (d, J = 2.3 Hz, 1H, H-9), 13.30 (bs, 1H, CO_2H). ^{13}C NMR (DMSO-d_6) δ 22.88, 25.02, 37.76, 66.99, 103.59, 105.70, 115.42, 119.97, 122.55, 123.29, 127.85, 128.54, 129.06, 136.00, 136.54, 139.18, 153.59, 157.91, 161.46, 166.37. HRMS (ESI) calcd for $C_{23}H_{22}NO_4S$ $(M+H)^+$ 408.12696, found 408.12689. Anal. calcd for $C_{23}H_{21}NO_4S$: C, 67.79; H, 5.19; N, 3.44. Found: C, 68.04; H, 5.44; N, 3.04.

4.1.5.6. 8-Methoxy-1-oxo-2-phenyl-1*H*-pyrido[2,1-*b*][1,3]benzothiazole-4-carboxylic acid (2e). The title compound was prepared according to the procedure used for compound **2c** starting from compound **8e**. Compound **2e** (65%) was obtained as white solid: mp 277–278 °C; ^{1}H NMR (400 MHz, DMSO-d_6) δ 3.80 (s, 3H, CH_3), 7.20 (dd, J = 2.5 and 8.6 Hz, 1H, H-7), 7.15–7.40 (m, 3H, Ar-H), 7.70–7.75 (m, 2H, Ar-H), 7.90 (d, J = 8.6 Hz, 1H, H-6), 8.10 (s, 1H, H-3), 8.80 (d, J = 2.5 Hz, 1H, H-9), 13.25 (bs, 1H, CO_2H). ^{13}C NMR (DMSO-d_6) δ 56.03, 104.99, 111.35, 114.93, 120.35, 122.34, 123.22, 127.77, 128.53, 129.06, 136.24, 136.67, 139.21, 153.12, 158.38, 161.48, 166.60. HRMS (ESI) calcd for $C_{19}H_{14}NO_4S$ $(M+H)^+$ 352.06436, found 352.06413. Anal. calcd for $C_{19}H_{13}NO_4S$: C, 64.95; H, 3.73; N, 3.99. Found: C, 64.67; H, 3.45; N, 4.37.

4.1.5.7. 8-Fluoro-1-oxo-2-phenyl-1*H*-pyrido[2,1-*b*][1,3]benzothiazole-4-carboxylic acid (2f). The title compound was prepared according to the procedure used for compound **2c** starting from compound **8f**. After the purification by column chromatography, eluting with $CHCl_3$/MeOH (9:1), compound **2f** (74%) was obtained as pale yellow solid: mp 326–328 °C; ^{1}H NMR (DMSO-d_6) δ 7.20–7.46 (m, 4H, H-7 and Ar-H), 7.55–7.65 (m, 2H, Ar-H), 7.90–8.10 (m, 2H, H-3 and H-7), 8.87 (dd, J = 2.7 and 11.2 Hz, 1H, H-9), 13.35 (bs, 1H, CO_2H). ^{13}C NMR (DMSO-d_6) δ 107.30 (d, $J_{C\text{-}F}$ = 30.8 Hz, C-9), 115.00 (d, $J_{C\text{-}F}$ = 23.7 Hz, C-7), 122.72, 124.33 (d, $J_{C\text{-}F}$ = 9.5 Hz, C-6), 125.01, 127.925, 128.60, 129.03, 136.43, 136.45, 138.85 (d, $J_{C\text{-}F}$= 14 Hz, C-9a), 153.21, 159.49, 161.37, 164.18 (d, $J_{C\text{-}F}$ = 459 Hz, C-8). HRMS (ESI) calcd for $C_{18}H_{11}FNO_3S$ $(M+H)^+$ 340.04437, found 340.04403. Anal. calcd for $C_{18}H_{10}FNO_3S$: C, 63.71; H, 2.97; N, 4.13. Found. C, 63.93; H, 3.19; N, 3.73.

4.1.6. Sodium salt of 8-(cyclohexyloxy)-1-oxo-2-phenyl-1*H*-pyrido[2,1-*b*][1,3]benzothiazole-4-carboxylic acid 5,5-dioxide (3c)

m-CPBA (0.08 g, 0.48 mmol) was added to a cooled solution of compound **2c** (0.10 g, 0.24 mmol) in mixture of CH_2Cl_2/acetone (15 mL, 2:1). The reaction mixture was stirred at room temperature for 24 h, then a saturated solution of $NaHCO_3$ (10 mL) was added and the mixture concentrated under reduced pressure. The precipitate formed was collected by filtration, washed with water and dried. After treatment of the solid with Et_2O, compound **3c** (0.02 g, 20%) was obtained as yellow sodium salt; ^{1}H NMR (400 MHz, DMSO-d_6) δ 1.25–1.45 (m, 6H, cyclohexyl CH_2), 1.65–1.75 and 1.95–2.00 (each m, 2H, cyclohexyl CH_2), 4.40–4.60 (1H, m, cyclohexyl CH), 7.15 (dd, J = 2.2 and 8.7 Hz, 1H, H-7), 7.35–7.50 (m, 3H, Ar-H), 7.60–7.70 (m, 2H, Ar-H), 7.87 (s, 1H, H-3), 8.00 (d, J = 8.7 Hz, 1H, H-6), 8.55 (d, J = 2.2 Hz, 1H, H-9). ^{13}C NMR (DMSO-d_6): 23.36, 25.38, 31.32, 75.90, 106.80, 115.26, 119.89, 121.49, 123.96, 128.59, 128.98, 129.19, 135.45, 135.77, 135.93, 138.62, 139.47, 159.73, 162.48, 162.82. HRMS (ESI) calcd for $C_{24}H_{21}NNaO_6S$ $(M+H)^+$ 474.09873,

found 474.09899. Anal. calcd for $C_{24}H_{20}NNaO_6S$: C, 60.88; H, 4.26; N, 2.96. Found: C, 61.03; H, 4.47; N, 2.60.

4.1.6.1. 8-Methoxy-1-oxo-2-phenyl-1*H*-pyrido[2,1-*b*][1,3]benzothiazole-4-carboxylic acid 5,5-dioxide (3e). The title compound was prepared according to the procedure used for compound **3c** starting from compound **2e**. The free carboxylic acid, obtained after treatment with 2 N HCl, was collected and washed with Et_2O to give compound **3e** (78%) as yellow solid: mp 308–312 °C (decompose); ^{1}H NMR (400 MHz, DMSO-d_6) δ 3.90 (s, 3H, OCH_3) 7.20 (dd, J = 2.2 and 8.7 Hz, 1H, H-7), 7.35–7.45 (m, 3H, Ar-H), 7.65–7.75 (m, 2H, Ar-H), 7.90 (s, 1H, H-3), 8.05 (d, J = 8.7 Hz, 1H, H-6), 8.60 (d, J = 2.2 Hz, 1H, H-9), 14.25 (bs, 1H, CO_2H). ^{13}C NMR (DMSO-d_6) δ 56.77, 105.77, 111.63, 114.45, 118.25, 124.35, 128.69, 129.27, 129.49, 134.91, 136.10, 136.15, 136.58, 142.52, 159.50, 163.12, 164.91. HRMS (ESI) calcd for $C_{19}H_{14}NO_6S$ $(M+H)^+$ 384.05419, found 384.05395. Anal. calcd for $C_{19}H_{13}NO_6S$: C, 59.52; H, 3.42; N, 3.65. Found: C, 59.85; H, 3.75; N, 3.31.

4.1.6.2. Sodium salt of 8-fluoro-1-oxo-2-phenyl-1*H*-pyrido[2,1-*b*][1,3]benzothiazole-4-carboxylic acid 5,5-dioxide (3f). The title compound was prepared according to the procedure used for compound **3c** starting from compound **2f** (47%) as yellow sodium salt; ^{1}H NMR (400 MHz, DMSO-d_6) δ 7.35–7.45 (m, 3H, Ar-H), 7.60 (dt, J = 1.9 and 8.5 Hz, 1H, H-7), 7.70–7.75 (m, 2H, Ar-H), 7.95 (s, 1H, H-3), 8.30 (dd, J = 5.7 and 8.5 Hz, 1H, H-6), 8.85 (dd, J = 1.9 and 10.9 Hz, 1H, H-9). ^{13}C NMR (DMSO-d_6) δ 108.15 (d, J_{C-F} = 30.2 Hz, C-9), 11.95, 116.30 (d, J_{C-F} = 23.5 Hz, C-7), 122.87 (d, J_{C-F} = 5.3 Hz, C-9a), 125.35 (d, J_{C-F} = 10.5 Hz, C-6), 128.74, 128.23, 129.61, 134.74, 135.97, 136.09, 136.74, 141.99, 159.40, 163.04, 165.50 (d, J_{C-F} = 250.6 Hz, C-8). HRMS (ESI) calcd for $C_{18}H_{10}FNNaO_5S$ $(M+H)^+$ 394.01615, found 394.01603. Anal. calcd for $C_{18}H_9FNNaO_5S$: C, 54.97; H, 2.31; N, 3.56. Found: C, 55.26; H, 2.60; N, 3.53.

4.2. NS5B enzymatic assay

The cloned gene for HCV 1b NS5BΔC21 was kindly provided by Dr. Joachim Jaeger, Astbury Centre, RepliZyme Ltd, UK. Recombinant HCV NS5B was expressed in *Escherichia coli* and purified by FPLC chromatography through DEAE and HyperD Heparin columns. Assays were performed as follows: NS5B (25–50 nM) was incubated in a final volume of 25 μL in the presence of 50 mM Tris–HCl pH 8.0, 1 mM DTT, 0.25 mg/mL BSA, 0.25 μM (3′-OH ends) of the RNA/RNA homopolymeric template (rA)40/(rU)20, 0.25 mM $MnCl_2$ and 2 μM [^{3}H]-UTP (37 Ci/mmol). Samples were incubated 40 min at 25 °C. Twenty microlitre aliquots were spotted on DE-81 filters (Wathman) which were washed twice in 0.5 M K_2HPO_4, once in water and once in acetone. Bound radioactivity was detected by liquid scintillation counter (MicrobetaTrilux, Perkin-Elmer). When inhibitors were tested, they were incubated 5 min on ice together with the enzyme and the RNA template, before addition of the [^{3}H]-UTP and subsequent incubation at 25 °C as described above.

4.3. Anti-HCV activity and cytostatic effect

One day before addition of compound, Huh 5.2 cells, containing the hepatitis C virus genotype 1b I389luc-ubi-neo/NS3-3′/5.1 replicon[32] and sub-cultured in cell growth medium [DMEM (Cat. No. 41965039) supplemented with 10% FCS, 1% non-essential amino acids (11140035), 1% penicillin/streptomycin (15140148) and 2% Geneticin (10131027); Invitrogen] at a ratio of 1:3–1:4 and grown for 3–4 days in 75cm^2 tissue culture flasks (Techno Plastic Products), were harvested and seeded in assay medium (DMEM, 10% FCS, 1% non-essential amino acids, 1% penicillin/streptomycin) at a density of six 500 cells/well (100 μL/well) in 96-well tissue culture microtiter plates (Falcon, Beckton Dickinson for evaluation of anti-metabolic effect and CulturPlate, Perkin Elmer for evaluation of anti-viral effect). The microtiter plates were incubated overnight (37 °C, 5% CO_2, 95–99% relative humidity), yielding a non-confluent cell monolayer.

The evaluation of the anti-metabolic as well as the anti-viral effect of each compound was performed in parallel. Four-step, 1-to-5 compound dilution series were prepared. Following assay setup, the microtiter plates were incubated for 72 h (37 °C, 5% CO_2, 95–99% relative humidity).

For the evaluation of anti-metabolic effects, the assay medium was aspirated, replaced with 75 μL of a 5% MTS (Promega) solution in phenol red-free medium and incubated for 1.5 h (37 °C, 5% CO_2, 95–99% relative humidity). Absorbance was measured at a wavelength of 498 nm (Safire^2, Tecan) and optical densities (OD values) were converted to percentage of untreated controls.

For the evaluation of anti-viral effects, assay medium was aspirated and the cell monolayers were washed with PBS. The wash buffer was aspirated, 25 μL of GloLysis Buffer (Cat. No. E2661, Promega) was added after which lysis was allowed to proceed for 5 min at room temperature. Subsequently, 50 μL of Luciferase Assay System (Cat. No. E1501, Promega) was added and the luciferase luminescence signal was quantified immediately (1000 ms integration time/well, Safire^2, Tecan). Relative luminescence units were converted to percentage of untreated controls.

The EC_{50} and EC_{90} (values derived from the dose–response curve) represent the concentrations at which, respectively, 50% and 90% inhibition of viral replication would be observed. The CC_{50} (value derived from the dose-response curve) represent the concentration at which the metabolic activity of the cells would be reduced to 50% of the metabolic activity of untreated cells.

A concentration of compound is considered to elicit a genuine anti-viral effect in the HCV replicon system when, at that particular concentration, the anti-replicon effect is well above the 70% threshold at concentrations where no anti-metabolic activity is observed.

4.4. Molecular docking experiments

The crystal structure of NS5B RdRp complexed with the inhibitor **9** (PDB ID 2BRK)[28] and **10** (PDB ID 3FRZ)[30] were retrieved from the RCSB Protein Data Bank and used as target for our modeling studies on TSI and II, respectively. Water molecules, except those involved in mediating hydrogen bonds between the ligands and the protein, were deleted. Schrödinger Protein Preparation Wizard[33] was then used to obtain a satisfactory starting structure for docking studies. This facility is designed to ensure chemical correctness and to optimize a protein structure for further analysis. In particular, hydrogen atoms were added, and bond orders and charges were assigned; the orientation of hydroxyl groups on Ser, Thr and Tyr, the side chains of Asn and Gln residues, and the protonation state of His residues were optimized. Steric clashes were relieved by performing a small number of minimization steps, not intended to minimize the system completely. In our study, the minimization (OPLSforce field) was stopped when the RMSD of the non-hydrogen atoms reached 0.30 Å.

Docking studies were performed using the software Glide version 5.0.[24–27] The prepared structures were used to generate the receptor grids, with no scaling for van der Waals radii of nonpolar receptor atoms. The grids were centered on the crystallographic positions of 9 for TSI and of 10 for TSII.

The structures of our hit compounds (**2b**, **2c** and **3c**) and the known NNIs **1**, **9** and **10** were constructed using the Schrödinger Maestro interface[34] and then submitted to Polak–Ribiere conjugate gradient minimization [0.0005 kJ/(Å mol) convergence]. The carboxylic acid moiety of the compounds was modelled as carboxylate, as predicted by MoKa.[29]

In our study, all compounds were flexibly docked in a stepwise manner with Glide SP (Standard Precision) and XP (Extra Precision) as scoring functions. Docking experiments were performed using 0.80 to scale the VdW radii of the nonpolar ligand atoms with a charge cutoff of 0.15. Two bound conformations per ligand were retained from SP docking, discarding poses as duplicates when rms deviation in the ligand-all atoms was less than 1.5 Å and maximum atomic displacement was less than 2.3 Å. The obtained docking poses where then refined, rescored and minimized using GlideXP. The best XP scoring bound conformation for each ligand was retained.

Acknowledgments

This work has been supported by Fondazione Cassa di Risparmio di Perugia (ricerca di base 2009, C.P.: 2009.010.00413). We are grateful to Roberto Bianconi, Stijn Delmotte, Mieke Flament and Tom Bellon for excellent technical assistance.

References and notes

1. Shepard, C. W.; Finelli, L.; Alter, M. *J. Lancet Infect. Dis.* **2005**, *5*, 558.
2. Bostan, N.; Mahmood, T. *Crit. Rev. Microbiol.* **2010**, *36*, 91.
3. Brown, R. S. *Nature* **2005**, *436*, 973.
4. Zeuzem, S.; Berg, T.; Moeller, B.; Hinrichsen, H.; Mauss, S.; Wedemeyer, H.; Sarrazin, C.; Hueppe, D.; Zehnter, E.; Manns, M. P. *J. Viral Hepat.* **2009**, *16*, 75.
5. Delang, L.; Coelmont, L.; Neyts, J. *Viruses-Basel* **2010**, *2*, 826.
6. Lange, C. M.; Sarrazin, C.; Zeuzem, S. *Aliment. Pharmacol. Ther.* **2010**, *32*, 14.
7. Flisiak, R.; Parfieniuk, A. *Expert. Opin. Investig. Drugs* **2010**, *19*, 63.
8. Opar, A. *Nat. Rev. Drug Disc.* **2010**, *9*, 501.
9. http://www.merck.com/newsroom/news-release-archive/prescription-medicine-news/2011_0513.html (accessed 09/20/2011).
10. http://investor.shareholder.com/vrtx/releasedetail.cfm?releaseid=573051 (accessed 09/20/2011).
11. Barreca, M. L.; Iraci, N.; Manfroni, G.; Cecchetti, V. *Future Med. Chem.* **2011**, *3*, 1027.
12. Watkins, W. J.; Ray, A. S.; Chong, L. S. *Curr.Opin. Drug Discov. Devel.* **2010**, *13*, 441.
13. Li, H.; Shi, S. T. *Future Med. Chem.* **2010**, *2*, 121.
14. Beaulieu, P. L. *Expert Opin. Ther. Pat.* **2009**, *19*, 145.
15. Hirashima, S.; Suzuki, T.; Ishida, T.; Noji, S.; Yata, S.; Ando, I.; Komatsu, M.; Ikeda, S.; Hashimoto, H. *J. Med. Chem.* **2006**, *49*, 4721.
16. Böhm, H.-J.; Flohr, A.; Stahl, M. *Drug Discovery Today* **2004**, *1*, 217.
17. Deore, R. R.; Chern, J. W. *Curr. Med. Chem.* **2010**, *17*, 3806.
18. Talele, T. *Curr. Bioac. Compd.* **2008**, *4*, 86.
19. Kato, T.; Chiba, T.; Okada, T. *Chem. Pharm. Bull.* **1979**, *27*, 1186.
20. Demolition of 2-methyl-5-phenoxy-1,3-benzthiazole exclusively gave the corresponding disulfide derivative which did not react with ethyl cyanoacetate.
21. Hodson, S. J.; Bishop, M. J.; Speake, J. D.; Navas, F., 3rd; Garrison, D. T.; Bigham, E. C.; Saussy, D. L., Jr.; Liacos, J. A.; Irving, P. E.; Gobel, M. J.; Sherman, B. W. *J. Med. Chem.* **2002**, *45*, 2229.
22. Chen, Y.; Bopda-Waffo, A.; Basu, A.; Krishnan, R.; Silberstein, E.; Taylor, D. R.; Talele, T. T.; Arora, P.; Kaushik-Basu, N. *Antiviral. Chem. Chemother.* **2009**, *20*, 19.
23. Beaulieu, P. L.; Bös, M.; Bousquet, Y.; Fazal, G.; Gauthier, J.; Gillard, J.; Goulet, S.; LaPlante, S.; Poupart, M. A.; Lefebvre, S.; McKercher, G.; Pellerin, C.; Austel, V.; Kukolj, G. *Bioorg. Med. Chem. Lett.* **2004**, *14*, 119.
24. Glide, version 5.6, Schrödinger, LLC, New York, NY, 2010.
25. Friesner, R. A.; Banks, J. L.; Murphy, R. B.; Halgren, T. A.; Klicic, J. J.; Mainz, D. T.; Repasky, M. P.; Knoll, E. H.; Shelley, M.; Perry, J. K.; Shaw, D. E.; Francis, P.; Shenkin, P. S. *J. Med. Chem.* **2004**, *47*, 1739.
26. Halgren, T. A.; Murphy, R. B.; Friesner, R. A.; Beard, H. S.; Frye, L. L.; Pollard, W. T.; Banks, J. L. *J. Med. Chem.* **2004**, *47*, 1750.
27. Friesner, R. A.; Murphy, R. B.; Repasky, M. P.; Frye, L. L.; Greenwood, J. R.; Halgren, T. A.; Sanschagrin, P. C.; Mainz, D. T. *J. Med. Chem.* **2006**, *49*, 6177.
28. Di Marco, S.; Volpari, C.; Tomei, L.; Altamura, S.; Harper, S.; Narjes, F.; Koch, U.; Rowley, M.; De Francesco, R.; Migliaccio, G.; Carfi, A. *J. Biol. Chem.* **2005**, *280*, 29765.
29. Milletti, F.; Storchi, L.; Sforna, G.; Cruciani, G. *J. Chem. Inf. Model.* **2007**, *47*, 2172.
30. Li, H.; Tatlock, J.; Linton, A.; Gonzalez, J.; Jewell, T.; Patel, L.; Ludlum, S.; Drowns, M.; Rahavendran, S. V.; Skor, H.; Hunter, R.; Shi, S. T.; Herlihy, K. J.; Parge, H.; Hickey, M.; Yu, X.; Chau, F.; Nonomiya, J.; Lewis, C. *J. Med. Chem.* **2009**, *52*, 1255.
31. Love, R. A.; Parge, H. E.; Yu, X.; Hickey, M. J.; Diehl, W.; Gao, J.; Wriggers, H.; Ekker, A.; Wang, L.; Thomson, J. A.; Dragovich, P. S.; Fuhrman, S. A. *J. Virol.* **2003**, *77*, 7575.
32. Vrolijk, J. M.; Kaul, A.; Hansen, B. E.; Lohmann, V.; Haagmans, B. L.; Schalm, S. W.; Bartenschlager, R. *J. Virol. Methods* **2003**, *110*, 201.
33. Schrödinger Suite 2010 Protein Preparation Wizard; Epik version 2.1, Schrödinger, LLC, New York, NY, 2010; Impact version 5.6, Schrödinger, LLC, New York, NY, 2010; Prime version 2.2, Schrödinger, LLC, New York, NY, 2010.
34. Maestro, version 9.2, Schrödinger, LLC, New York, NY, 2011.